ME570 Assignment 3

Zili Wang
zw2445@bu.edu

October 28, 2020

Contents

1 Notes

1.1 2D Sphere

sphere: a structure with fields - sphere.xCenter (coordinates of the sphere center); sphere.radius (radius>0 for filled-in sphere, radius<0 for hollow sphere); sphere.distInfluence (influence distance of the sphere)

Filled-in sphere:

$$d(x) = ||x - x_{center}|| - |r|$$
$$\nabla d(x) = \frac{x - x_{center}}{||x - x_{center}||}$$

Hollow sphere:

$$d(x) = |r| - ||x - x_{center}||$$
$$\nabla d(x) = -\frac{x - x_{center}}{||x - x_{center}||}$$

Basically, if the point is on the obstacle, its distance value if negative. Figure 1 gives the results of sphere_testCollision.m, where given a sphere with sphere.Xcenter= $[0; 0]$, sphere.radius= 1 for filled-in sphere, sphere.radius= -1 for hollow sphere, 100 randomly generated points are colored according to the sign of their distance from the sphere surface (red for negative<in collision>, green for positive<free>).

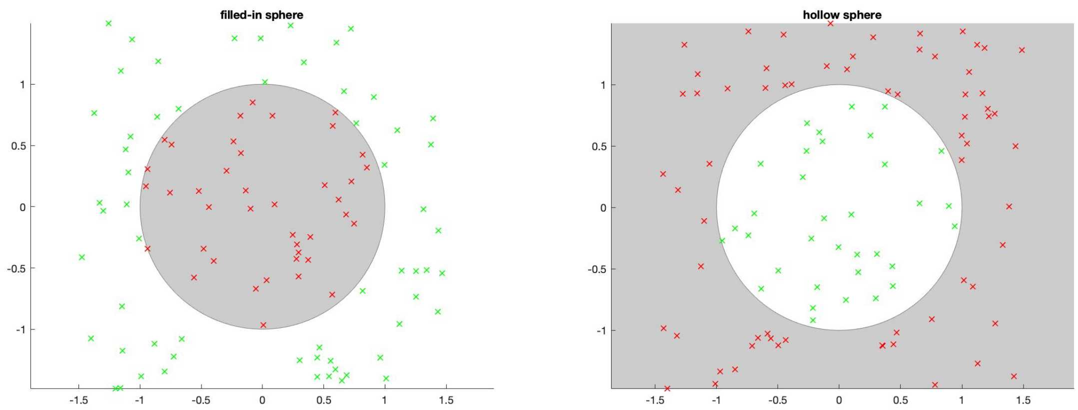

(a) Filled in Sphere

(b) Hollow Sphere

Figure 1: 2D Sphere With 100 Random Points

1.2 World

The sphere world work-space is as sphereworld.m, where 'world' contains sphere structures, xStart are the initial positions, xGoal are the goal locations. Figure 2 is the result of sphereworld_plot.m, which plots the obstacles and the goal locations as $*$.

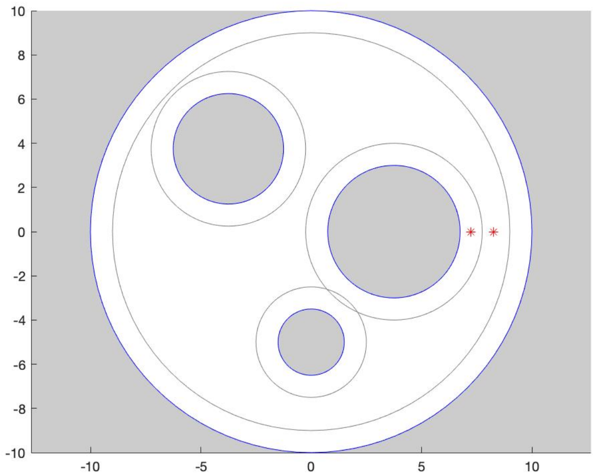

Figure 2: Configuration Space Collision Test

1.3 Potential-based Planner

world: a structure as in 'World'. potential: a structure with fields - potential.xGoal (goal location); potential.repulsiveWeight (weight of the attractive term w.r.t. the repulsive term); potential.shape (shape of attrative potential <'conic' or 'quadratic'>).

1.3.1 Attractive Potential

$$
\begin{aligned}
U_{attr} &= d^p(x, x_{goal}) = ||x - x_{goal}||^p \\
\nabla U_{attr} &= p d^{p-2}(x, x_{goal}) \frac{x - x_{goal}}{||x - x_{goal}||} \\
&= p d^{p-1}(x, x_{goal}) \frac{x - x_{goal}}{||x - x_{goal}||}
\end{aligned}
$$

where $p = 1, 2$ gives 'conic' and 'quadratic' shape respectively.

1.3.2 Repulsive Potential

$$U_{rep,i}(x) = \begin{cases} \frac{1}{2}(\frac{1}{d_i(x)} - \frac{1}{d_{influence}})^2 & \text{if } 0 < d_i(x) < d_{influence} \\ 0 & \text{if } d_i(x) > d_{influence} \\ NaN & \text{if } otherwise \end{cases}$$

$$\nabla U_{rep,i}(x) = \begin{cases} -(\frac{1}{d_i(x)} - \frac{1}{d_{influence}})\frac{1}{d_i(x)^2}\nabla d_i(x & \text{if } 0 < d_i(x) < d_{influence} \\ 0 & \text{if } d_i(x) > d_{influence} \\ NaN & \text{if } otherwise \end{cases}$$

1.4 Total Potential

$$U = U_{attr} + \alpha \sum_i U_{rep,i}$$

Figure 3, 4, 5 give the results of field_plotTest.m using field_plotThreshold.m, which contains the plot of the value and gradient of attractive and repulsive potential (obstacle 1,2), and the totol potential for the world. Noting the color bar is in log scale.

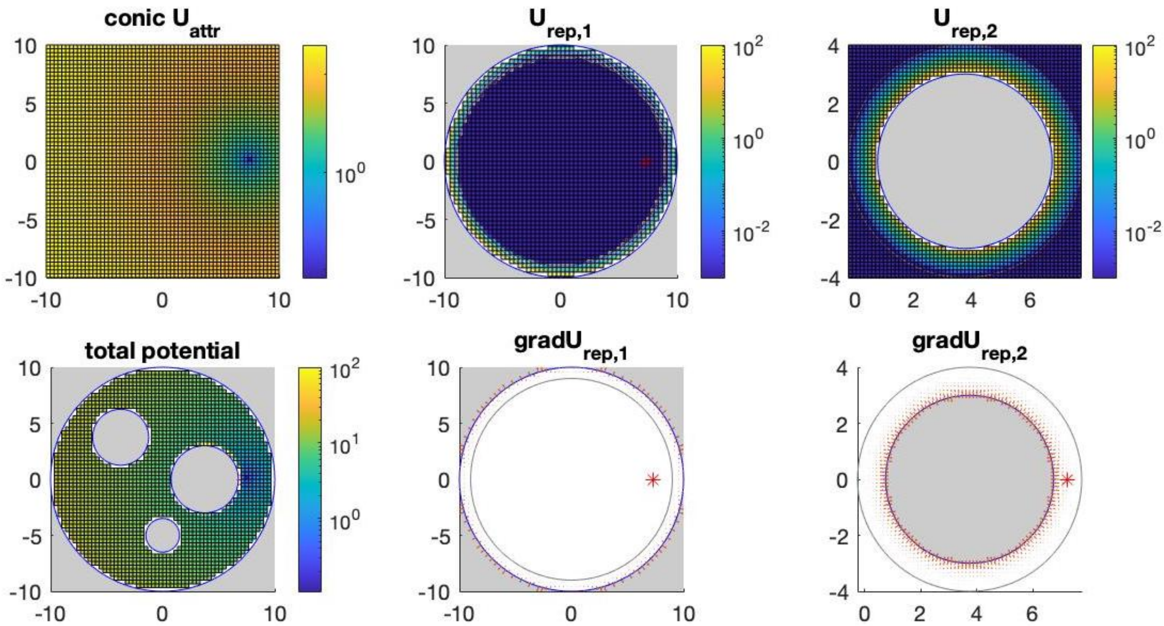

Figure 3: Conic Potential-based Planner

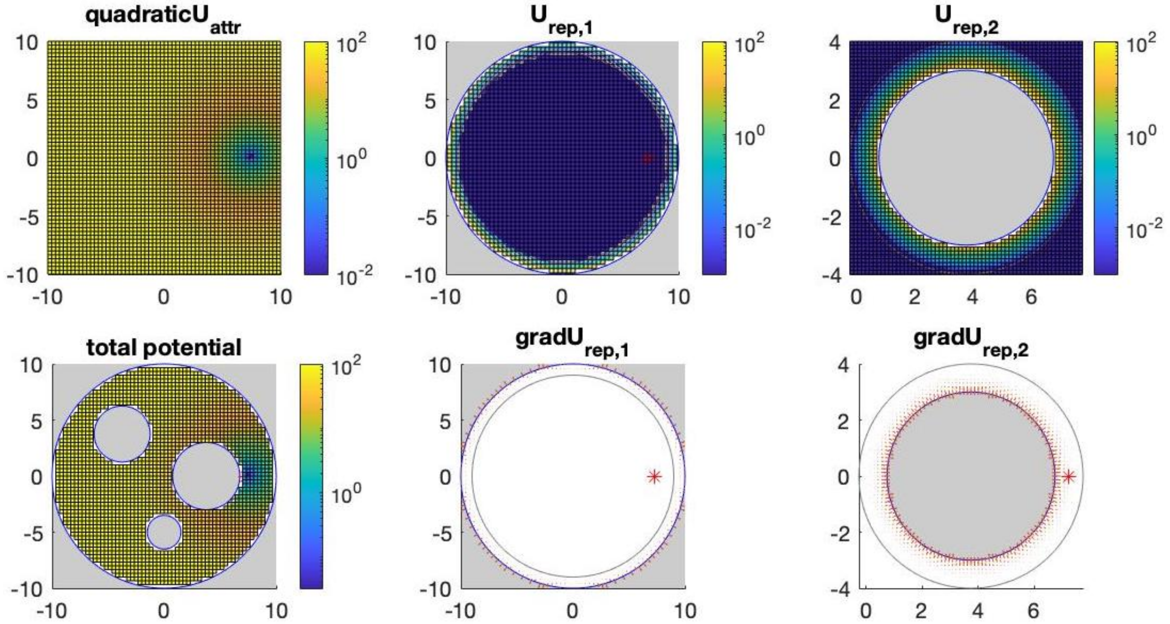

Figure 4: Quadratic Potential-based Planner

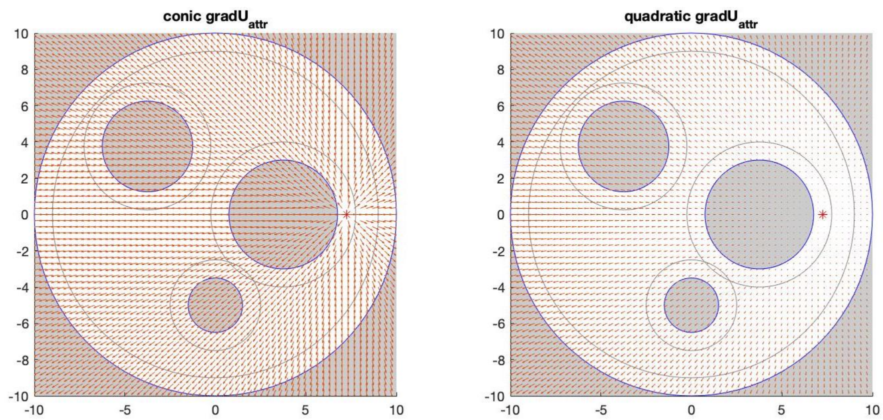

Figure 5: Gradient of Attractive Potential

2 Question 2.1

Figure 6, 7, 8, 9, 10 shows the results of potential_planner_runPlot.m. There are several comparisons:

- Figure 6 ($\epsilon = 0.01$) and 7($\epsilon = 0.1$): with other parameters being the same (conic $U_attr, \alpha = 0.1$), a larger step size ϵ gives a faster convergence to the final goal.
- Figure 6 (conic U_{attr}) and 8 (quadratic U_{attr}): with other parameters being same ($\alpha = 0.1, \epsilon = 0.01$), quadratic-shape attractive potential gives a faster convergence to the final goal.

- Figure 8 ($\alpha = 0.1$) and 9 ($\alpha = 50$): with other parameters being the same (quadratic $U_{attr}, \epsilon = 0.01$), a higher repulsive weight gives a slower convergence to the final goal, but it will also constrain the agent more away from the obstacle. Also, the final goal location inside the influence region cannot be reached with a higher α.
- Figure 9 ($\epsilon = 0.01$) and 10 ($\epsilon = 0.02$): with other parameters being the same (quadratic $U_{attr}, \alpha = 50$), a smaller step size can make a failure settings reach the goal again.

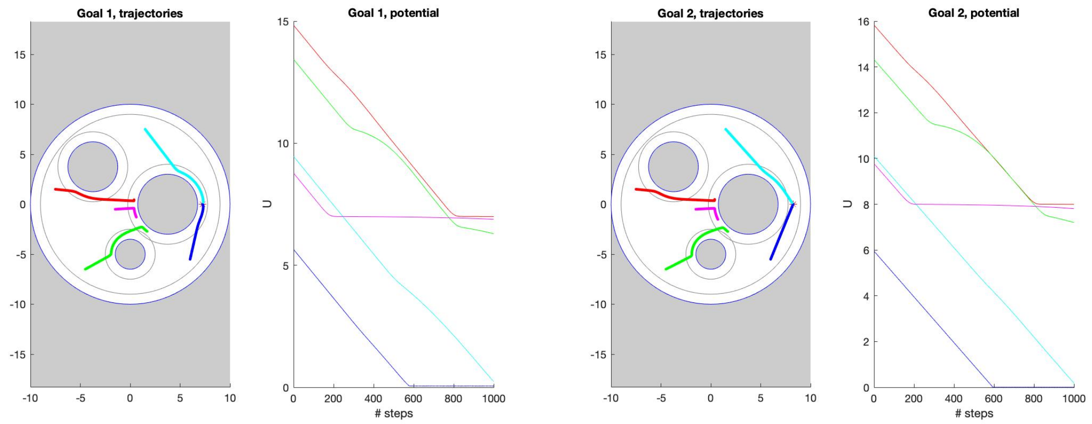

(a) Goal 1

(b) Goal 2

Figure 6: Conic U_{attr} with $\alpha = 0.1, \epsilon = 0.01$

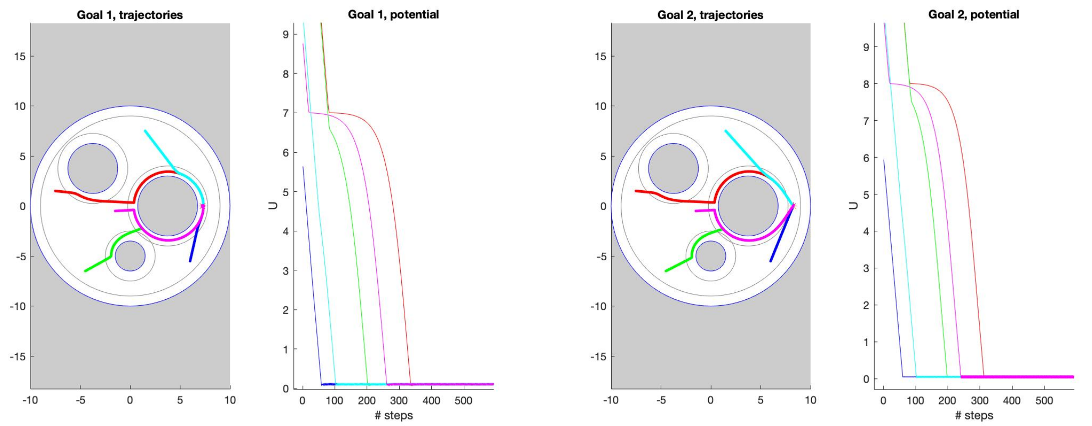

(a) Goal 1

(b) Goal 2

Figure 7: Conic U_{attr} with $\alpha = 0.1, \epsilon = 0.1$

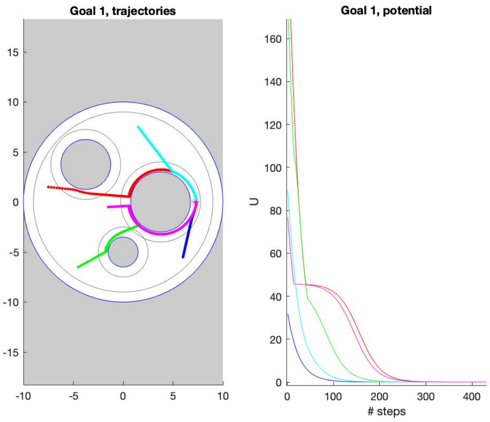

(a) Goal 1

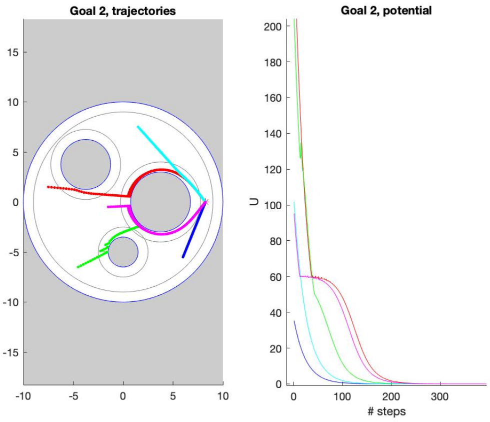

(b) Goal 2

Figure 8: Quadratic U_{attr} with $\alpha = 0.1, \epsilon = 0.01$

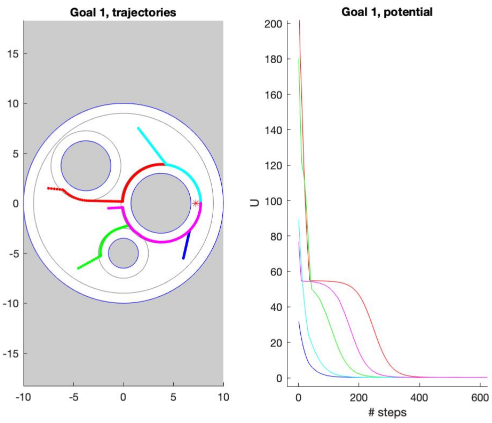

(a) Goal 1

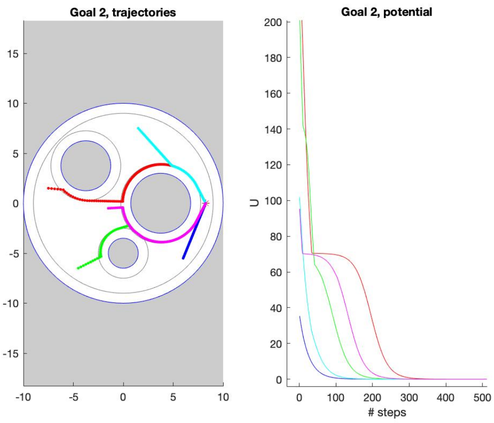

(b) Goal 2

Figure 9: Quadratic U_{attr} with $\alpha = 50, \epsilon = 0.01$

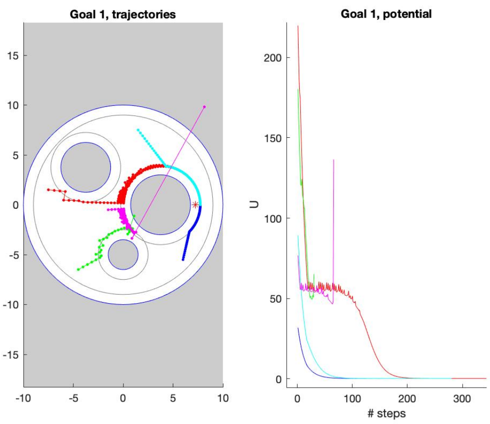

(a) Goal 1

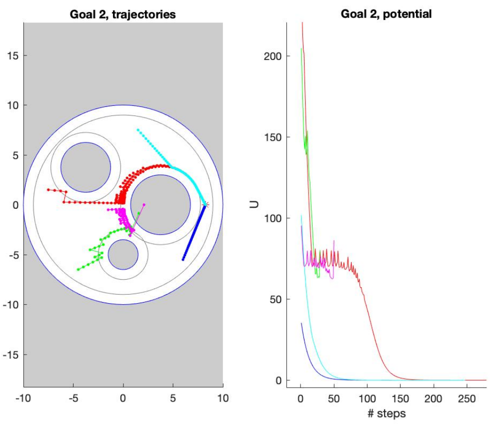

(b) Goal 2

Figure 10: Quadratic U_{attr} with $\alpha = 50, \epsilon = 0.02$

3 Question 2.2

Figure 11 gives the value and gradient plot of potential in Figure 6 and 7. Figure 12 gives the value and gradient plot of potential in Figure 8. And Figure 13 gives the value and gradient plot of potential in Figure 9 and 10. Noting that the color bar is in log scale. There are two comparisons:

- Figure 11 and 12: since the quadratic-shape attractive potential grows faster away from the goal location, with the same repulsive weight, the one with quadratic-shape gives larger portion of high value and gradient.
- Figure 12 and 13: since higher α makes the obstacle avoidance more concerned, it gives a sharper value change (gradient) as shown in Figure 13, especially when it is closer to the boundaries.

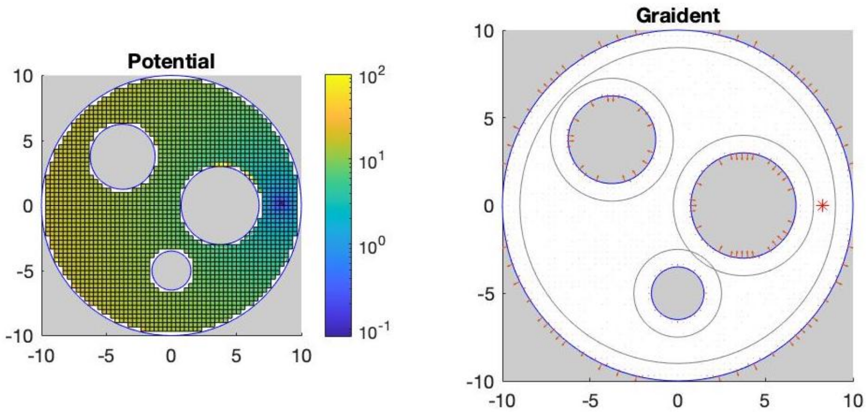

Figure 11: Conic $U_{attr}, \alpha = 0.1$

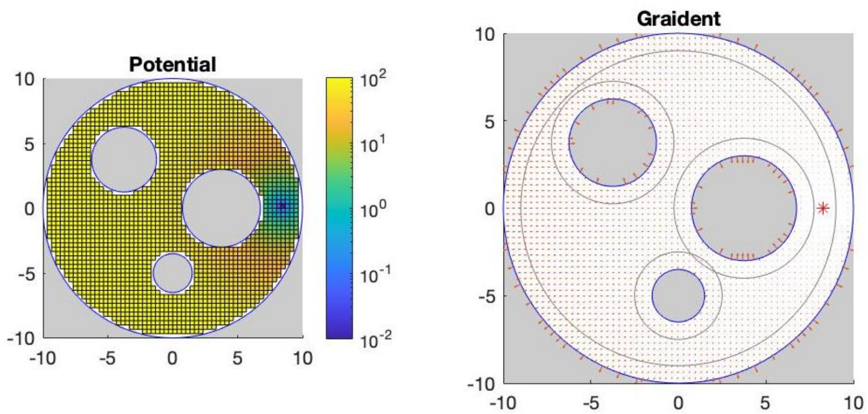

Figure 12: Quadratic $U_{attr}, \alpha = 0.1$

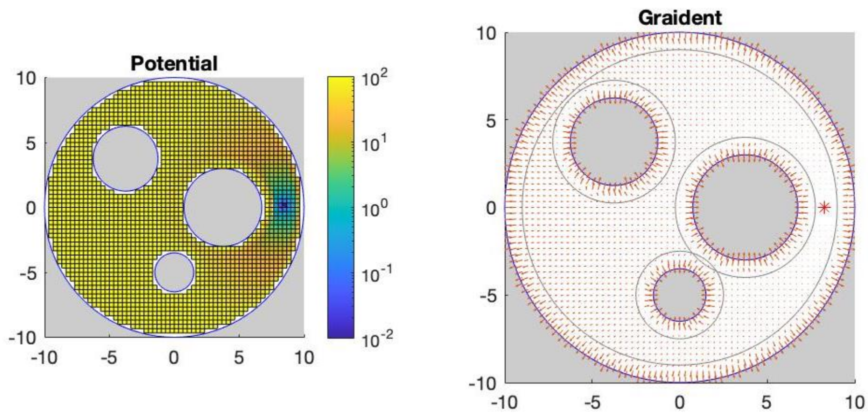

Figure 13: Quadratic U_{attr}, $\alpha = 50$

4 Question 2.3

As discussed in Question 2.1, increasing the epsilon makes the agent converge faster (larger step on the negative gradient direction makes it easier to reach the goal). Increasing the repulsive weight makes the agent easier to fail, while decreasing the step size simultaneously can balance the effect (greater repulsive weight makes the term involving collision avoidance larger, therefore harder to reach the goal location. A smaller epsilon can alleviate the effect by making the overall value smaller). Quadratic-shape attractive potential can converge faster comparing with the conic-shape attractive potential (quadratic-shape makes the potential change faster than conic-shape and has less chattering).

When repulsive weight is small, the effect of collision avoidance is less, so the agent is less constrained to move away from the obstacle. While if it is too large, the effect of collision avoidance dominates, the agent is less likely to move inside the influence region, and the free space is limited. In some case, without decreasing the epsilon, the agent can go crazy and the potential will not keep decreasing.

When epsilon is small, the agent takes longer time to converge and reach the goal location. If it is too large, the agent changes greatly and it may miss the optimal potential and has a chattering.

5 Question 2.4

If the planner correctly succeeded, the value of potential U will keep decreasing until reaching a near-zero/zero value toward the end of the iterations. If the planner failed, it can have sudden jump and not decrease the potential value all the time.

6 Question 2.5

Two goals are different in the way that goal 1 is inside the influence region of one obstacle, while goal 2 is outside. The quadratic-shape are more likely to fail comparing to conic-shape when the repulsive weight is large. It induces larger change (by comparing Figure 14 and 10).

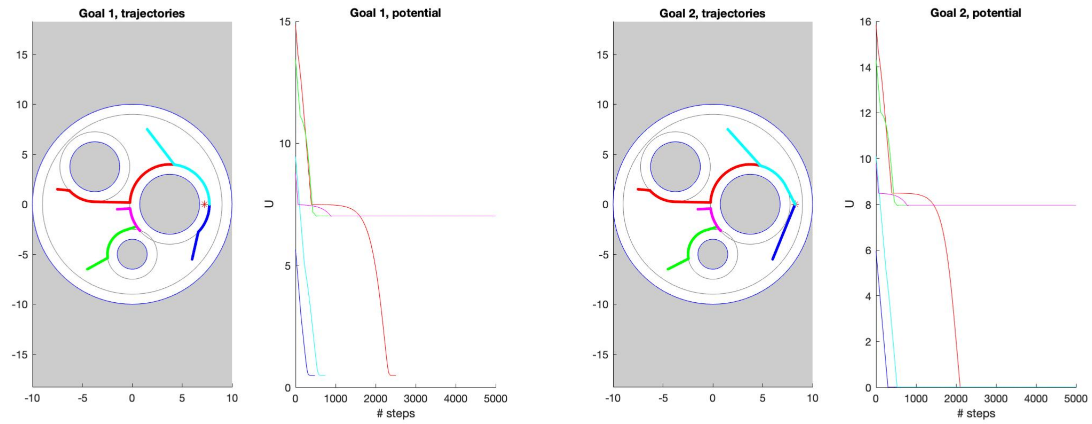

(a) Goal 1

(b) Goal 2

Figure 14: Conic U_{attr} with $\alpha = 50, \epsilon = 0.02$

7 Question 3.1

CLF constraint using $U_{attr}(x)$:

$$\begin{aligned}
&\dot{x} = 0 + I \cdot u \\
&\nabla U_{attr}^T f(x) + \nabla U_{attr}^T g(x) u + c_V U_{attr} \leq 0 \\
&\Rightarrow \nabla U_{attr}^T u + c_V U_{attr} \leq 0 \\
&\Rightarrow \nabla U_{attr}^T u + U_{attr} \leq 0
\end{aligned}$$

CBF constraint using $d_i(x)$:

$$\begin{aligned}
&\dot{x} = 0 + I \cdot u \\
&\nabla d_i^T f(x) + \nabla d_i^T g(x) u + c_h d_i \geq 0 \\
&\Rightarrow \nabla d_i^T u + c_h d_i \geq 0 \\
&\Rightarrow \nabla d_i^T u + d_i \geq 0
\end{aligned}$$

The QP problem is:

$$\begin{aligned} u^*(x) = \arg\min_{u,\xi} \quad & ||u||^2 + m\delta^2 \\ \text{s.t.} \quad & U_{attr}^T u + U_{attr} \leq \delta \\ & -\nabla d_i^T u - d_i \leq 0 \end{aligned}$$

8 Question 3.2

Figure 15 shows the results of clfcbf_control_Test.m, a QP using quadratic-shape U_{attr} as the CLF constraint, $d_i(x)$ as the CBF constraints, and it uses 20 control steps to reach the goals.

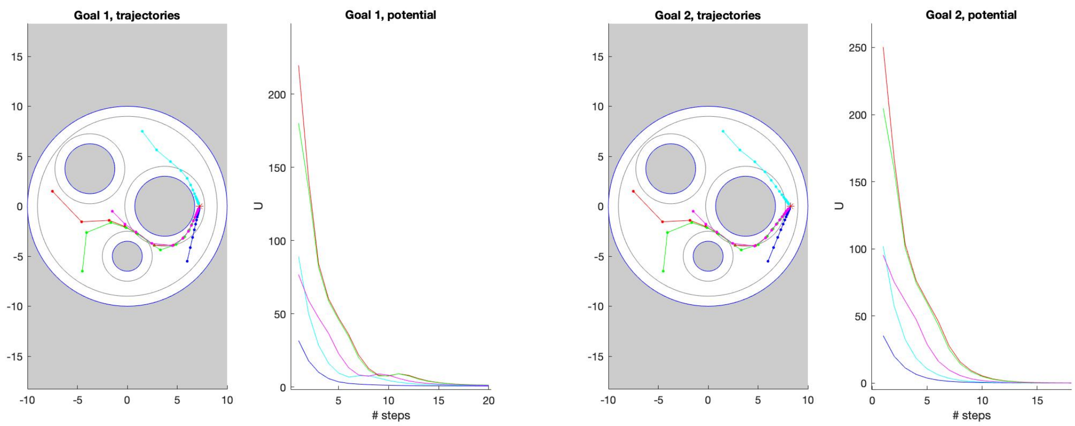

(a) Goal 1

(b) Goal 2

Figure 15: QP: Quadratic U_{attr} with $\alpha = 1, \epsilon = 0.5$

9 Question 3.3

Figure 16 shows the results of clfcbf_field_plotTest.m, a visualization of the control field $u^*(x)$ for the QP using quadratic-shape U_{attr} as the CLF constraint, $d_i(x)$ as the CBF constraints, and it uses 20 control steps to reach the goals.

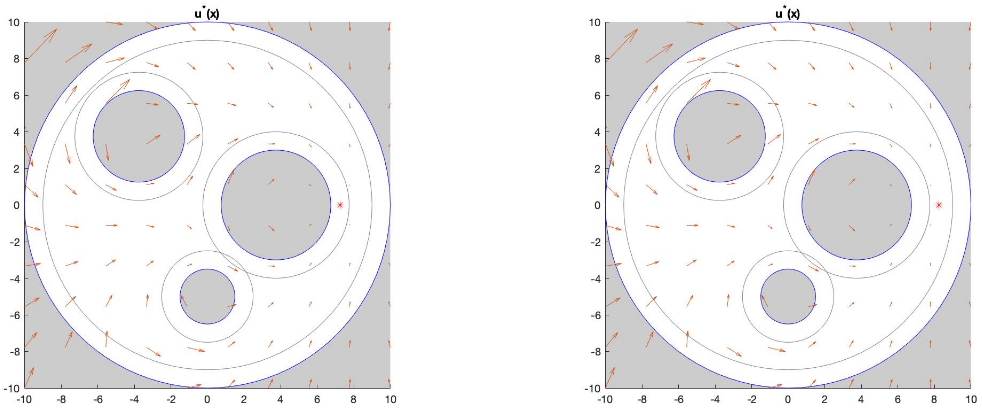

(a) Goal 1 (b) Goal 2

Figure 16: Control Field of QP: Quadratic U_{attr} with $\alpha = 1, \epsilon = 0.5$

10 Question 3.4

The CLF-CBF controller is to find a control that drives the agent to the goal while avoiding collisions. The slack variable δ makes the problem always feasible, with a cost to progress very slightly when the goal is close to the obstacle. Comparing to traditional gradient-based planner:

- Advantage: it is more general since it fits into the input-affine system. It works better and requires less steps.
- Disadvantage: Solving a QP is computationally more expensive. Running 20 steps using CLF-CBF controller consumes more time than running 5000 steps using gradient-based methods.

11 Question 4.1

$$
\begin{aligned}
{}^{W}p &= \begin{bmatrix} \cos(\theta_1+\theta_2)\ {}^{B_2}p_x - \sin(\theta_1+\theta_2)\ {}^{B_2}p_y + 5\cos(\theta_1) \\ \sin(\theta_1+\theta_2)\ {}^{B_2}p_x + \cos(\theta_1+\theta_2)\ {}^{B_2}p_y + 5\sin(\theta_1) \end{bmatrix} \\
&\downarrow\ {}^{B_2}p = [{}^{B_2}p_x; {}^{B_2}p_y] = {}^{B_2}p_{eff} = [5;0] \\
{}^{W}p_{eff} &= \begin{bmatrix} 5\cos(\theta_1+\theta_2) + 5\cos(\theta_1) \\ 5\sin(\theta_1+\theta_2) + 5\sin(\theta_1) \end{bmatrix} \\
\frac{d}{dt}({}^{W}p_{eff}) &= \begin{bmatrix} \frac{dp_x}{d\theta_1}\frac{d\theta_1}{dt} + \frac{dp_x}{d\theta_2}\frac{d\theta_2}{dt} \\ \frac{dp_y}{d\theta_1}\frac{d\theta_1}{dt} + \frac{dp_x}{d\theta_2}\frac{d\theta_2}{dt} \end{bmatrix} \\
&= \begin{bmatrix} -5\sin(\theta_1+\theta_2)(\dot{\theta_1}+\dot{\theta_2}) - 5\sin(\theta_1)\dot{\theta_1} \\ 5\cos(\theta_1+\theta_2)(\dot{\theta_1}+\dot{\theta_2}) + 5\cos(\theta_1)\dot{\theta_1} \end{bmatrix} \\
&= \begin{bmatrix} -5\sin(\theta_1+\theta_2) - 5\sin(\theta_1) & -5\sin(\theta_1+\theta_2) \\ 5\cos(\theta_1+\theta_2) + 5\cos(\theta_1) & 5\cos(\theta_1+\theta_2) \end{bmatrix} \begin{bmatrix} \dot{\theta_1} \\ \dot{\theta_2} \end{bmatrix} \\
J &= \begin{bmatrix} -5\sin(\theta_1+\theta_2) - 5\sin(\theta_1) & -5\sin(\theta_1+\theta_2) \\ 5\cos(\theta_1+\theta_2) + 5\cos(\theta_1) & 5\cos(\theta_1+\theta_2) \end{bmatrix}
\end{aligned}
$$

Another way to think is:

$$
\begin{aligned}
{}^{W}p_{eff} &= R(\theta_1+\theta_2)\ {}^{B_2}p_{eff} + R(\theta_1)\begin{bmatrix} 5 \\ 0 \end{bmatrix} \\
\frac{d}{dt}(R(\theta_1+\theta_2)) &= \begin{bmatrix} 0 & -(\dot{\theta_1}+\dot{\theta_2}) \\ (\dot{\theta_1}+\dot{\theta_2}) & 0 \end{bmatrix} R(\theta_1+\theta_2) \\
&= \begin{bmatrix} 0 & -1 \\ 1 & 0 \end{bmatrix} R(\theta_1+\theta_2)\ (\dot{\theta_1}+\dot{\theta_2}) \\
\frac{d}{dt}(R(\theta_1)) &= = \begin{bmatrix} 0 & -1 \\ 1 & 0 \end{bmatrix} R(\theta_1)\ \dot{\theta_1} \\
\frac{d}{dt}({}^{W}p_{eff}) &= \begin{bmatrix} 0 & -1 \\ 1 & 0 \end{bmatrix} \{[R(\theta_1+\theta_2) + R(\theta_1)]\dot{\theta_1} + R(\theta_1+\theta_2)\dot{\theta_2}\} \begin{bmatrix} 5 \\ 0 \end{bmatrix}
\end{aligned}
$$

which gives the same answer.

12 Question 4.1 (Optional)

The diary file to compare the results of two functions is imported as below:

```
theta=[0;1];
thetaDot=[1;0];
twolink_jacobianMatrix(theta)*thetaDot

ans =

   -4.2074
    7.7015

twolink_jacobian(theta, thetaDot)

ans =

   -4.2074
    7.7015
```

13 Question 4.2

Figure 17 shows the results of twolink_planner_Test.m, which describes the behaviors of two-link Manipulator with Quadratic U_{attr} and $\alpha = 0.005$, $\epsilon = 0.0005$. While other starting points can succeed with higher α and ϵ values, starting point 5 has less choice and can only survive with small parameter values.

$$
\begin{aligned}
{}^{W}p_{eff} &= R(\theta_1+\theta_2)\ {}^{B_2}p_{eff} + R(\theta_1)\begin{bmatrix}5\\0\end{bmatrix}\\
&\rightarrow U({}^{W}p_{eff}(\theta))\\
\frac{d}{dt}U({}^{W}p_{eff}(\theta)) &= \frac{d}{dp}U^T(p_{eff})\frac{d\,p_{eff}}{dt}\\
&= \nabla_p U^T(p_{eff})J\dot{\theta}\\
&= \nabla_\theta U^T\dot{\theta}\\
\nabla_\theta U &= J^T\nabla_p U
\end{aligned}
$$

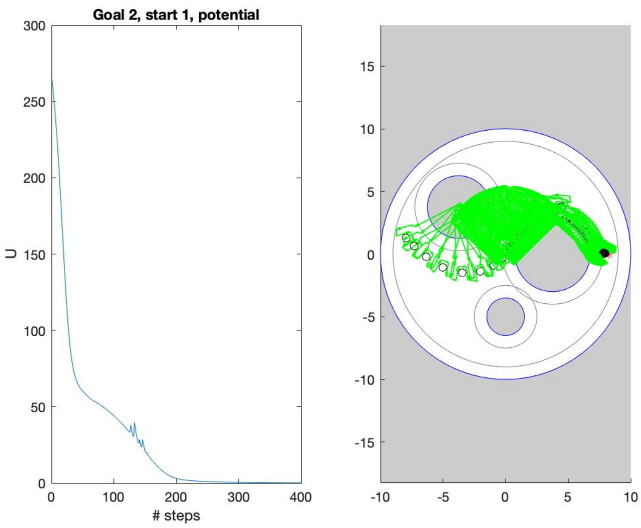

(a) Starting Point 1

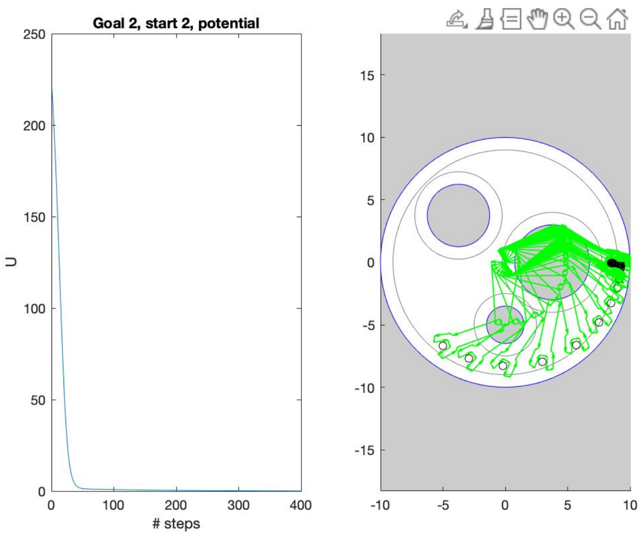

(b) Starting Point 2

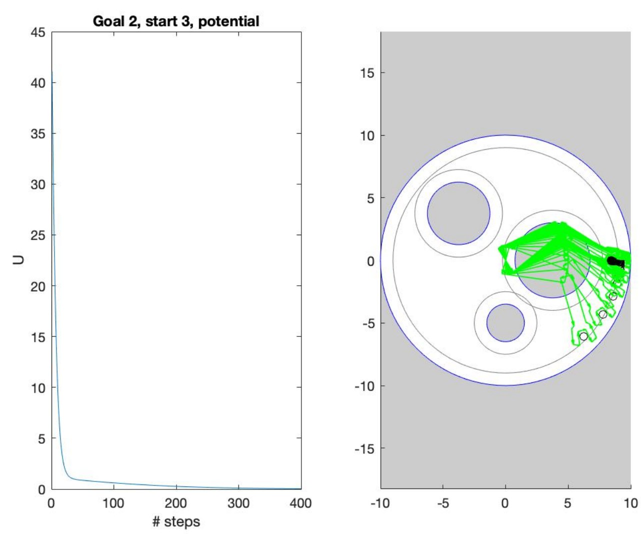

(c) Starting Point 3

Figure 17: Two-link Manipulator: Quadratic U_{attr} with $\alpha = 0.005, \epsilon = 0.0005$

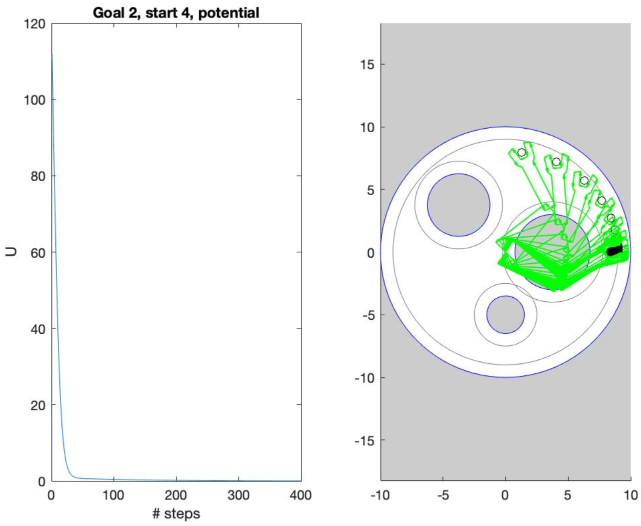

(d) Starting Point 4

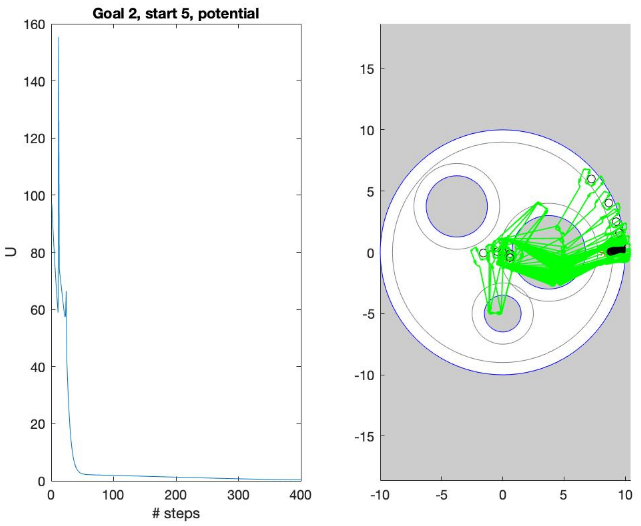

(e) Starting Point 5

Figure 17: Two-link Manipulator: Quadratic U_{attr} with $\alpha = 0.005$, $\epsilon = 0.0005$ (cont.)

14 Question 5.1

- Code and Debug: 5.5 hours
- Report: 2 hours
- Total: 7.5 hours
- Simple: Some implementations are based on previous homework
- Difficult: A comprehensive analysis of the relationship between different parameters, and results.